JOURNAL OF MATERIALS SCIENCE **35** (2000) 2675–2681

Subtle changes in magnetic Barkhausen noise before the macroscopic elastic limit*

C. G. STEFANITA, L. CLAPHAM, D. L. ATHERTON
Department of Physics, Queen's University, Kingston, Ontario K7L 3N6, Canada
E-mail: lynann@physics.queensu.ca

A mild steel specimen was loaded in tension up to ≈0.4% strain, with Magnetic Barkhausen Noise (MBN) measurements made at increasing strain levels. In addition, an MBN investigation was performed on a mild steel specimen bent progressively to ≈0.2% longitudinal surface strain. Overall, the parameter termed 'MBN_{energy}' increased significantly in the elastic, yet remained basically unchanged in the plastic range of deformation. While still in the elastic range, particular strain levels displayed abrupt changes in the MBN_{energy}. Variations in scatter about the average MBN_{energy} value, as well as distinct modifications in pulse height distributions, occurred simultaneously with the abrupt changes in MBN_{energy}. The non-uniform stress distribution among grains in the polycrystalline samples initiated dislocation formation in some grains before extending to other grains. Dislocation strain fields contributed to redistribution of strain within a grain leading to non-uniform changes in magnetic texture. Results indicate that the magnetic Barkhausen noise technique can detect microyielding.

1. Introduction

Despite extensive research [1–3], the complex effects of stress on ferromagnetic behaviour are not yet fully understood. The study of stress influences on polycrystalline ferromagnetic materials resists reduction to a precisely formulated set of problems solvable by experimental investigation or mathematical analysis. The situation is complicated by the fact that the strain caused by stress can be either elastic or plastic, with different mechanisms responsible for both. Furthermore, the grains within a polycrystalline sample deform differently depending on their crystallographic orientation with respect to the direction of applied stress, and this can lead to non-uniform changes in magnetic texture.

Magnetic Barkhausen noise (MBN) is known to be stress dependent [3–11]. MBN is associated with the abrupt, irreversible motion of domain walls overcoming pinning sites as a ferromagnetic sample is magnetized. It occurs primarily in the mid field range of the magnetic hysteresis curve where domain wall motion is the dominant magnetization mechanism. Although MBN sensitivity to stress is well known and has been exploited for at least three decades, these earlier investigations focussed primarily on the overall trends observed as specimens were subjected to deformation [5–8]. However, the inherent anisotropic deformation of grains gives rise to subtle changes in MBN at strain levels below the elastic limit, and the present paper investigates this behaviour.

2. Theoretical background

The formation of magnetic domains in a ferromagnetic material results from the minimization of the sum of five energy terms—[3]—exchange, magnetostatic, magnetoelastic, magnetocrystalline, and a domain wall energy term. Among these energy terms, magnetocrystalline energy plays a significant role. When the domain magnetization is aligned with certain crystallographic directions, the magnetocrystalline energy is a minimum. These preferred directions are called 'axes of easy magnetization', and are along ⟨100⟩ in iron.

The application of a magnetic field changes the magnetostatic energy, altering the overall energy balance, with the other energies readjusting to minimize their sum. The combined effort of the five energies to maintain a minimum leads to domain wall displacement, with magnetic domains having magnetization vectors most closely aligned with the applied field increasing in size at the expense of less favourably oriented domains [4]. However, domain walls are not completely free to move in response to an applied magnetic field. Wall displacement can be temporarily retarded by local pinning sites such as dislocation tangles, inclusions, and grain boundaries. Movement of domain walls across these pinning sites requires energy, and makes the process irreversible. This phenomenon gives rise to the Barkhausen effect [3].

An applied magnetic field is likely to affect simultaneously several domains within a grain, or in

*Research supported by Natural Sciences and Engineering Research Council of Canada, Gas Research Institute and Pipetronix Ltd.

neighbouring grains with similar crystallographic orientation. Consequently, domain wall movement becomes a correlated event, producing a 'Barkhausen cluster'. Various authors have examined correlated domain wall motion or cluster formation [9, 12–14], which appears to be material dependent [15]. The ability to develop clusters relies to a great extent on demagnetizing effects during Barkhausen transitions [4, 15]. Eddy current generation is less significant in harder ferromagnetic materials (investigated in the present study), thereby cluster development should not be impeded by demagnetizing fields in these materials. Crystallographic texture is expected to favour cluster formation through correlated domain wall motion in neighbouring grains with similar orientation.

An applied stress can create domain wall motion without the application of a magnetic field [3]. Stress effects on single-domain cubic crystals have been treated theoretically by various authors [4, 10, 16, 17]. Even though their formulations use different approaches, the final mathematical expressions are similar. The arguments are based on the minimization of the five energies. In the absence of an applied magnetic field, the magnetostatic energy of a nonmagnetized ferromagnet is zero. In the presence of only one domain, neither exchange energy nor wall energy play a role. Therefore, when a stress is acting, both magnetocrystalline and magnetoelastic energy compete to determine the direction of the domain magnetization

$$\begin{aligned} E_{\text{magnetocrystalline}} + E_{\text{magnetoelastic}} &= K\left(\xi_1^2\xi_2^2 + \xi_2^2\xi_3^2 + \xi_3^2\xi_1^2\right) \\ &\quad - \frac{3}{2}\lambda_{100}\sigma\left(\xi_1^2\gamma_1^2 + \xi_2^2\gamma_2^2 + \xi_3^2\gamma_3^2\right) \\ &\quad - 3\lambda_{111}\sigma(\xi_1\xi_2\gamma_1\gamma_2 + \xi_2\xi_3\gamma_2\gamma_3 + \xi_3\xi_1\gamma_3\gamma_1) \quad (2.1) \end{aligned}$$

where ξ_1, ξ_2, ξ_3 are the direction cosines of the domain magnetization with respect to crystal axes, and γ_1, γ_2, γ_3 are the direction cosines of the applied stress σ with respect to crystal axes. The above expression was derived for a deformed simple cubic lattice [4, 10] for which the crystallographic directions ⟨100⟩ and ⟨111⟩ are possible magnetic easy axis directions. The saturation magnetostrictions along ⟨100⟩ (easy axis direction in iron) and ⟨111⟩ (easy axis direction in nickel) are represented by λ_{100}, and λ_{111}, respectively, and K represents the anisotropy constant. Qualitatively, the direction of domain magnetization is determined by the magnitude of K versus $\frac{3}{2}\lambda_{100}\sigma$ and $3\lambda_{111}\sigma$. Given the measured values [13] $\lambda_{100} = 19.5 \times 10^{-6}$, and $\lambda_{111} = -18.8 \times 10^{-6}$, an elastic stress of ≈1660 MPa is necessary to overcome the effect of the magnetocrystalline energy, and change the direction of domain magnetization from ⟨100⟩. The yield strength of the steel investigated in the present work was ≈206 MPa, therefore domain magnetization vectors remain parallel to ⟨100⟩ (easy axis direction in iron) even under an applied stress.

The analysis can be extended qualitatively to a multidomain single crystal. Since a simple realignment with the stress direction is not energetically favourable, the domain configuration minimizes its energy through domain wall displacement. As a result, a change in the volume of magnetic domains takes place. A more energetically favourable domain configuration is achieved if domains lying closest to the direction of applied tensile stress grow at the expense of domains with other magnetization directions [4]. In this manner, the magnetoelastic energy of the system is decreased.

A recent study involving a multidomain single crystal [11] suggests a modification in the number of 180° domain walls in response to an applied stress. For those domains lying closest to the stress direction, a tensile stress creates an increase in the 180° domain wall population, and a compressive stress a decrease. The contributions of the applied stress to the domain configuration are evaluated in terms of changes in magnetoelastic energy, 180° domain wall area and energy. The 'critical level' of an applied tensile stress for which the addition of another domain wall becomes favourable was calculated for pipeline steel. The calculated stress values (between 32 and 290 MPa) are common [11].

It should be noted that an analysis of polycrystalline materials rests only qualitatively on the theoretical arguments described above.

3. Experimental technique

3.1. Loading configurations

The sample investigated was a 3 mm thick mild steel plate for which a qualitative crystallographic texture analysis was conducted prior to MBN measurements. Pole figures were constructed for the (110), (200), and (211) peaks. These indicated a random distribution of crystallographic planes. The engineering stress-strain curve was measured on an Instron Tensile Testing Machine under strain control, using a cross head speed of 0.008 mm/s. This indicated a yield point of ≈206 MPa (determined by a 0.2% offset method), with a Young's modulus of 167 GPa. Strain gauges were mounted on specimens to measure the strain in the applied stress direction. The strain gauges were cycled seven times prior to establishing the zero strain reading.

Both uniaxial and bending stress experiments were performed. In the uniaxial case, tensile samples of central dimensions 297 mm (L) × 57 mm (W) × 3 mm (T) were mounted in the jaws of a uniaxial stressing device with a maximum load capacity of 180 kN. The specimen was designed such that the stress axis was along the rolling direction of the plate. The maximum stress that could be obtained on the stressing device for this specimen was 976 MPa, well beyond the yield point of 206 MPa. A region of ≈150 mm length on the specimen surface was carefully ground to a 1000 SiC grit finish, thus producing a flat, oxide-free surface for MBN measurements. Stress was applied to the specimen in increments, with MBN measurements taken at each new stage of deformation. Measurements were performed in the elastic and plastic ranges of deformation, up to a total of ≈0.4% strain.

The bending experiment employed a rectangular beam sample 1220 mm (L) × 127 mm (W) × 3 mm (T) with the beam axis directed along the rolling direction of the plate. A 610 mm long region was sanded to a

1000 SiC grit finish. The beam was bent by two equal and opposite couples acting in the same longitudinal plane, achieved by hanging two equal loads on either end of the beam which was supported at points approximately 25% from each end. The beam was deformed progressively in steps, to a longitudinal surface strain of ≈0.2%, and then progressively unloaded. MBN measurements were performed for each loading and unloading stage. The surface plastic strain present after the removal of the external load was 0.06%.

3.2. Magnetic barkhausen noise detection

Fig. 1 shows a block diagram of the experimental apparatus. An exciter coil wound on a C-shaped ferrite core and driven by a 12 Hz sinusoidal source magnetizes the specimen. The drive is amplified by a bipolar power supply before reaching the exciter coil. The MBN signal is detected by a read head placed between the pole pieces of the ferrite core. The output of the detector is fed to a preamplifier with a gain of 2000, and through a band-pass filter of 3–200 kHz. Data is collected and analyzed on a PC digital oscilloscope board (Computerscope). The MBN signal is sampled at intervals of 1 μs for 16 ms with a buffer size of 16 K. The estimated depth of minimum penetration of the magnetizing field is roughly 1 mm, whereas the depth from which the MBN signal originates is ≈30 μm (according to skin depth considerations [4]).

Two types of axial scans were made across the specimens—in the first, the magnetic excitation field was directed parallel and, in the second, transverse to the sample axis.

Most studies use different magnetic Barkhausen noise parameters to analyze the overall signal. The parameters used in the present paper for MBN signal analysis are 'MBN_{energy}' and pulse height distributions. The MBN signal at any given measurement position consists of a collection of voltage pulses or 'events' of varying amplitudes. Only voltage pulses with amplitudes above 125 mV were considered in the analysis.

The MBN_{energy} is obtained by calculating the time integral of the squared voltage pulse. An 'average MBN_{energy}' is obtained by calculating the mean of the MBN_{energy} over all measured positions. The deviation of each MBN_{energy} value from the mean is averaged over all measured positions and is termed 'scatter in MBN_{energy}'.

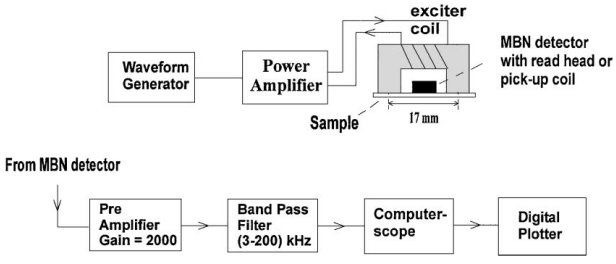

Figure 1 Block diagram of experimental apparatus for producing and detecting magnetic Barkhausen noise.

4. Results

4.1. Steel sheet uniaxially loaded in tension

The parameter MBN_{energy} was analyzed as a function of position along the sample axis, for progressive uniaxial deformation to 0.23%. Results for a detector orientation parallel to the applied axis are presented in Fig. 2. This figure indicates that, at a given strain level, the MBN_{energy} is fairly consistent along the sample length. Furthermore, an increase in axial strain is accompanied by a corresponding increase in MBN_{energy} at all positions. Although not shown, the data for the transverse detector orientation shows an opposite trend—a decreasing MBN_{energy} with increasing strain. These general trends are consistent with previously reported data [7, 8].

A summary of the MBN_{energy} variation with deformation is shown in Fig. 3, by plotting MBN_{energy} values averaged over all positions as a function of strain for both detector orientations. As seen in the diagram, there is significant change in MBN_{energy} with strain in the elastic region, yet little variation in the plastic regime. Notable features are the abrupt changes in MBN_{energy} values before the macroscopic yield point—specifically a drop is observed at 0.09% for the parallel detector orientation, with a concurrent increase in MBN_{energy} in the tranverse detector orientation. A further decrease

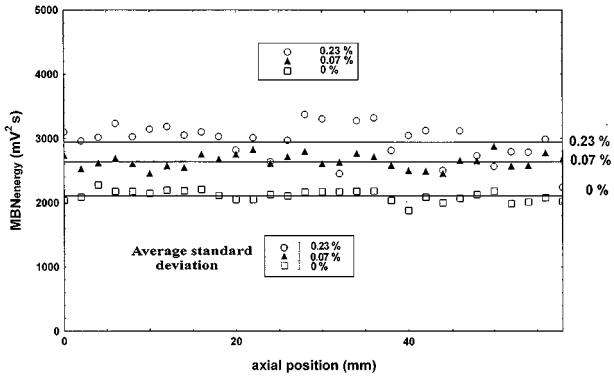

Figure 2 Variation of MBN_{energy} as a function of position along applied stress axis of uniaxially deformed specimen for selected strain levels. Detector oriented parallel to the axis. Average MBN_{energy} value are marked by solid, parallel lines.

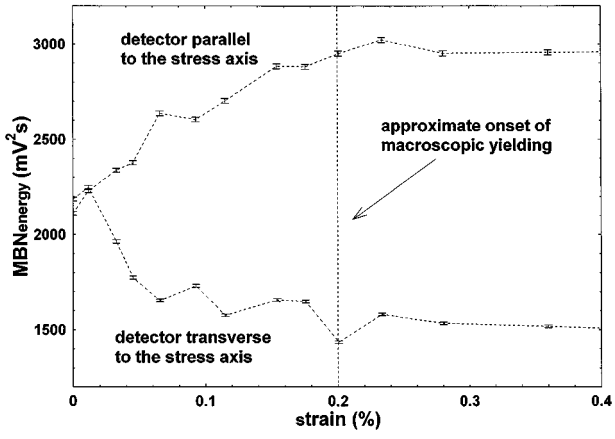

Figure 3 Summary of average MBN_{energy} data as a result of axial scans performed on the uniaxially deformed specimen. Connecting dashed lines are only for guidance.

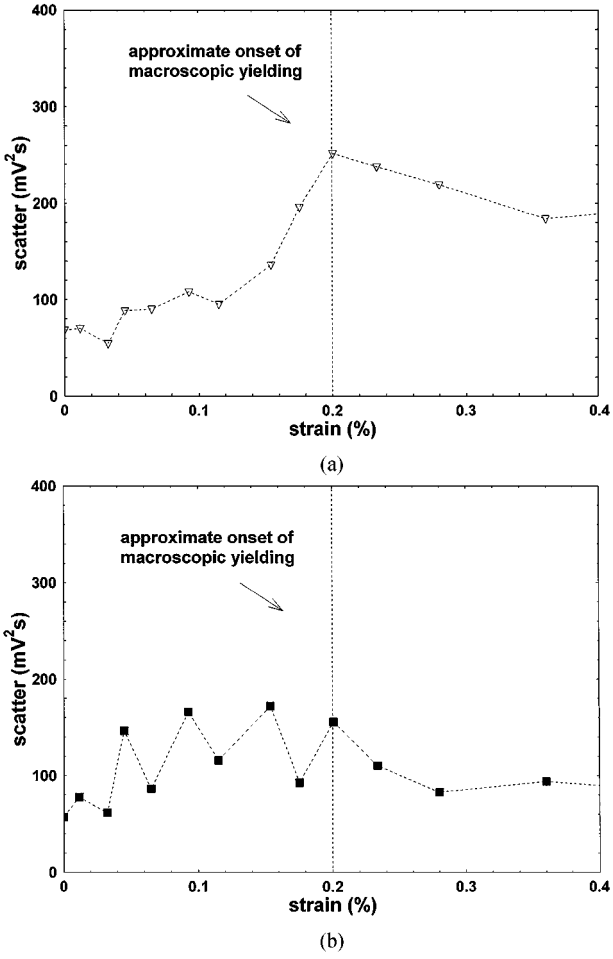

Figure 4 Variation with strain of MBN_{energy} scatter for a detector oriented (a) parallel, and (b) transverse to the applied stress direction. Measurements were performed on the uniaxially deformed specimen. Connecting dashed lines are only for guidance.

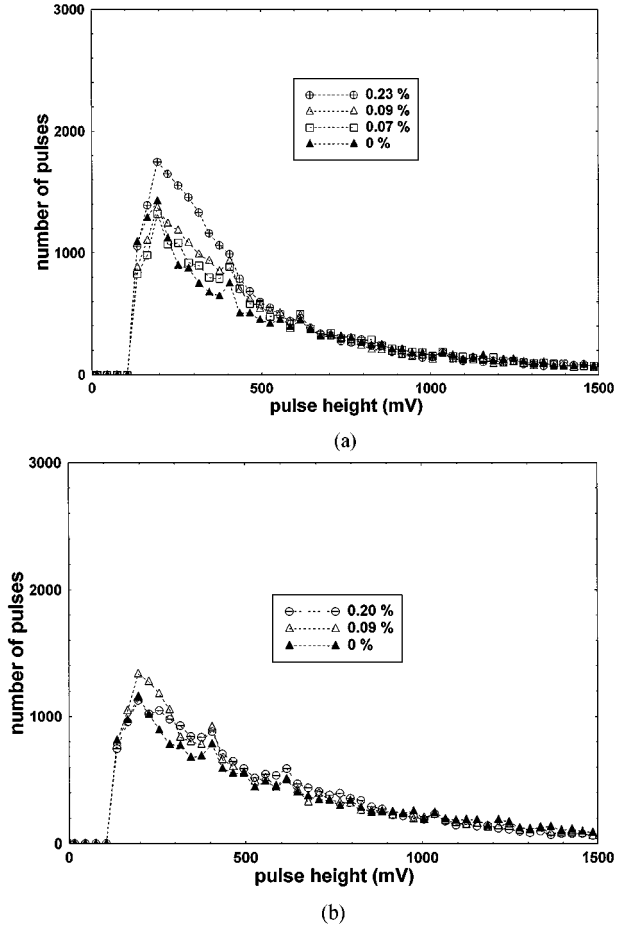

Figure 5 Pulse height distributions for a detector oriented (a) parallel, and (b) transverse to the applied stress direction. Measurements performed on the uniaxially deformed specimen. Selected strain levels are presented.

is observed at 0.20% strain for the transverse detector orientation.

Fig. 2 also indicates the MBN_{energy} scatter with position for each strain level. Fig. 4a and b illustrate how this scatter varies with increasing strain. Overall, the scatter increases with strain up to the yield point for the parallel detector orientation (Fig. 4a), while in the transverse direction a trend is not easily recognized (Fig. 4b). Similar to average MBN_{energy} behaviour shown in Fig. 3, the elastic and plastic regions demonstrate different patterns in MBN_{energy} scatter.

Changes in the MBN parameters described above can be correlated with evident modifications in the pulse height distributions, shown in Fig. 5a and b, for detector orientations parallel and transverse to stress, respectively. The first variations in the shape of the pulse height distribution curves become apparent above 0.07% strain (Fig. 5a), with a slight increase in the number of intermediate voltage pulses. This effect is more notable at 0.09% strain (Fig. 5a) that corresponds to the drop in Fig. 3 discussed earlier. The increase in MBN_{energy} at 0.23% (Fig. 2) coincides with a rise in the pulse height distribution curve in the low as well as intermediate voltage range. Above this deformation level measurements show little variation in the shape of the distribution curve.

Of note is the result for the detector oriented transverse to the stress direction. Despite the overall decrease in average MBN_{energy} values with increased strain (Fig. 3), the number of intermediate voltage pulses is noted to increase (Fig. 5b).

4.2. Beam in bending

For the detector oriented parallel to the beam axis, the MBN_{energy} is seen to increase (Fig. 6), a result consistent with observations described in the previous section. The transverse direction exhibits almost no variation in MBN_{energy}, however subtle changes in MBN_{energy} occur with increased strain.

The scatter in MBN_{energy} follows an irregular pattern for both detector orientations (Fig. 7).

5. Discussion

As mentioned in Section 2, the magnetoelastic energy of a particular domain configuration is minimized when the domains most closely aligned with the stress direction increase in size at the expense of less favourably oriented domains. Neighbouring magnetic domains with the same orientation with respect to the stress direction experience similar volume changes.

Plastic deformation distorts the lattice permanently by ‘slipping’ when the critical resolved shear stress

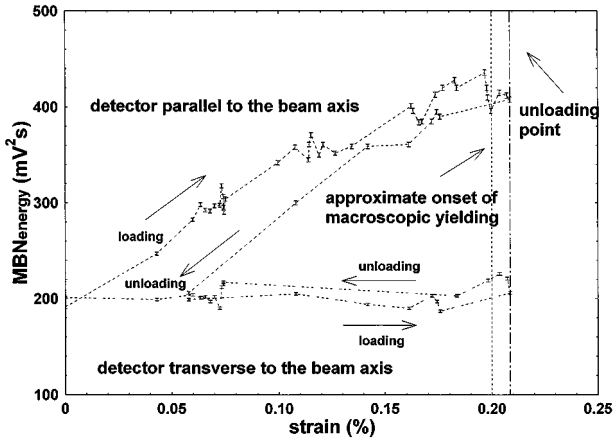

Figure 6 Summary of average MBN_{energy} data as a result of axial scans performed on the beam in bending. Connecting dashed lines are only for guidance.

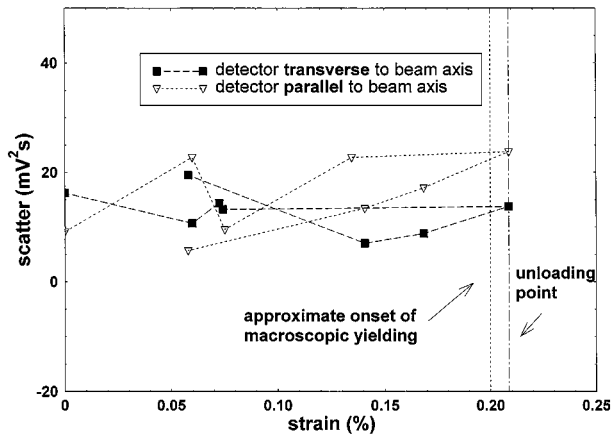

Figure 7 Variation with strain of MBN_{energy} scatter. Measurements performed on the beam in bending. Only a few strain levels were analyzed for scatter. Connecting dashed lines are only for guidance.

is reached on a slip plane. A dislocation is formed at the boundary between a slipped and unslipped portion of the plane. The interplanar spacing is altered in the vicinity of the dislocation, creating a strain field. The dislocation-induced strain fields give rise to nonuniform changes in the volume of magnetic domains.

An applied stress acting simultaneously on grains with different crystallographic orientations leads to longitudinal or shear incompatibility at grain boundaries [18]. The type of incompatibility depends on the relative orientation of the grains with respect to each other. Longitudinal incompatibility occurs for crystallographic orientations such as [100] and [111] [19]. In the case of longitudinal incompatibility, one grain is in tension, while its neighbour is in compression. This affects the changes in volume of magnetic domains in the two grains.

Elastic stresses between grains are accommodated by dislocations generated in grain boundary regions, thereby reducing stress concentration. This is supported by experimental evidence obtained by transmission electron microscopy [20, 21], and etchpitting techniques [22–25]. Early signs of plastic deformation, termed microyielding, are associated with dislocation generation before the macroscopic yield point is reached. By comparison, macroscopic yielding is characterized by massive dislocation generation and motion. The resulting additional strain fields alter the intragranular stress distribution and thereby magnetic domain sizes. In addition, increased dislocation densities impede the simultaneous motion of domain walls. At this stage, there is little further increase in MBN signal.

The stress at grain boundaries due to longitudinal incompatibility is almost three times higher than the critical resolved shear stress within the grain [26]. The higher stress levels at grain boundaries are likely to cause dislocations to be generated first in grain boundary regions, before they form in the grain interior. Consequently, magnetic domains in the vicinity of grain boundaries are affected differently than those in the grain interior. An increase in volume of magnetic domains located in grain boundary regions is likely to occur at the expense of their neighbours. An example of how this might occur is shown in Fig. 8. Fig. 8a

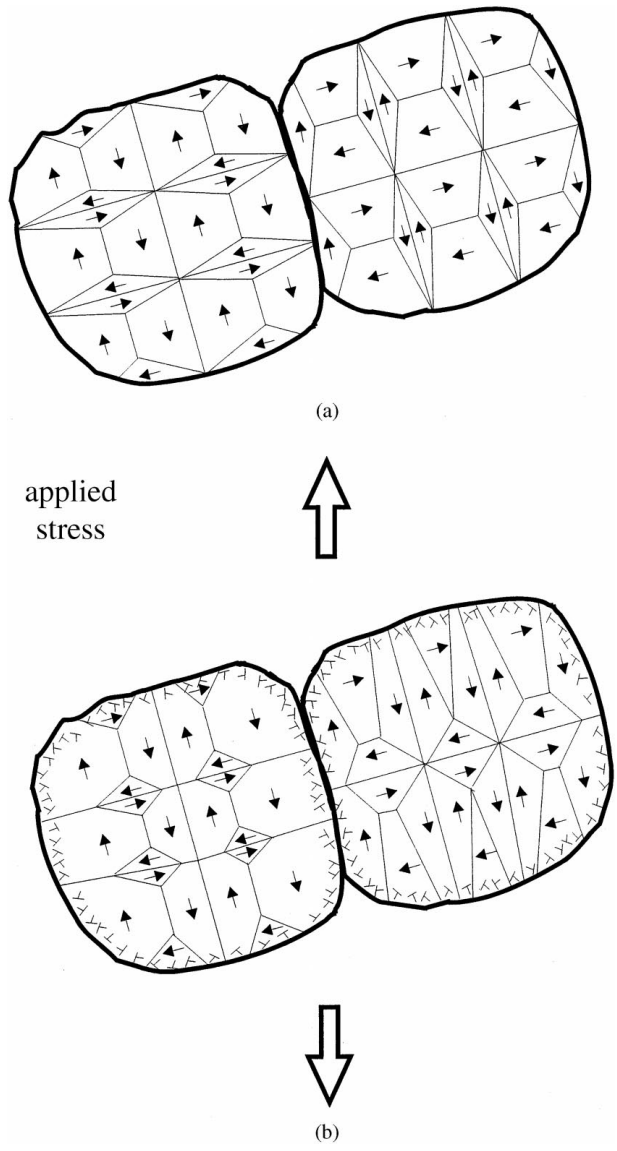

Figure 8 Hypothesized magnetic domain configurations in polycrystalline iron (a) before the application of stress (b) after the applied stress initiates dislocation formation at grain boundaries. No magnetic field is applied.

is a schematic illustration of a possible domain wall distribution in the absence of stress, while Fig. 8b corresponds to the distribution following microyielding. In this figure, both grains are shown to be affected by a tensile stress producing dislocation initiation in both grains. However, dislocations are not generated simultaneously in all grains at a particular stress level. While some grains develop dislocations at a certain stress level, dislocation initiation does not occur in other grains until higher stress levels.

On these grounds, the overall MBN signal is expected to be affected by an applied tensile stress in the following manner: As discussed, during *elastic stress* those domains with magnetizations most closely aligned with the direction of tensile stress increase in size at the expense of neighbouring domains with less favourable orientations. Furthermore, magnetic domains experiencing similar increases in volume are likely to become simultaneously active under an applied field. This increases the MBN response. In addition, there is an increased number of 180° domain walls in the tensile stress direction [11] which contribute to an enhanced signal. The observed rise in signal is displayed both by the uniaxially loaded specimen (Fig. 3), and beam in bending (Fig. 6), the latter subjected to a tensile elastic stress on the outer surface.

The abrupt MBN signal changes in the elastic region are believed to be a result of *microyielding* phenomena. With the onset of microyielding, dislocations form in grain boundary regions in some grains. The strain fields created contribute to further size increases in magnetic domains located in grain boundary regions. The MBN response of the latter is expected to be greater than the response of smaller size domains in the grain interior. However, depending on how many grains develop dislocations, a certain overall MBN signal is obtained. In addition, the unequal size increases between magnetic domains leads to differences in their energetic level. As a result, not all domains become active simultaneously under an applied field. The outcome of the diverse mechanisms that accompany microyielding leads to abrupt changes in MBN_{energy} values below the macroscopic yield point (Figs 3 and 6). Concurrently, other MBN parameters (scatter, pulse height distributions) display abrupt variations for strains below 0.2%, as seen in Figs 4, 5 and 7.

Plastic deformation of the bulk of the grain leads to added dislocation strain fields in the grain interior. These strain fields influence the stress distribution within grains contributing to changes in magnetic domain sizes. Dislocation tangles within grains cause impediments to simultaneous wall movement in neighbouring domains. As plastic deformation progresses into the bulk of the grain, the rate of increase in MBN_{energy} is reduced (Fig. 3 —above the macroscopic yield point).

An overall contrasting trend in MBN_{energy} is evidenced in the transverse direction compared to the applied stress direction. When subjected to a uniaxial tensile stress, the specimen experiences a transverse compressive strain due to the Poisson effect. Consequently, magnetic domains with magnetizations closely aligned with the transverse direction undergo a reduction in volume [4]. The MBN signal decreases in the direction transverse to the applied stress (Fig. 3), yet abrupt changes, again believed to be due to microyielding phenomena, are observed.

The specimen subjected to bending stresses seems to experience less transverse compressive strains, given the approximately unchanged MBN_{energy} values displayed in Fig. 6. This is likely due to the bending method used since loads applied at the two beam ends produce a force with a point of application on the beam axis. Given the relatively large beam width (127 mm), applied load effects are less significant at the transverse beam edges than along the central axis. Furthermore, the transverse compressive strain experienced in bending usually decreases with distance in from the edge [27]. A 17 mm long detector used for MBN scans performed along the beam axis would not detect transverse compressive stresses.

6. Conclusion

The application of a tensile stress significantly increased MBN_{energy} values in the elastic range. However, the MBN_{energy} remained essentially unchanged in the plastic deformation range up to ≈4% strain. This behaviour was ascribed to the combined effect of changes of magnetic domain sizes, increases in the number of 180° domain walls, and magnetic domains becoming simultaneously active.

The abrupt variations in average MBN_{energy} observed below the macroscopic elastic limit were attributed to dislocation formation in grain boundary regions at different strain levels. Concurrently, inconsistent trends in scatter about the average MBN_{energy} value, and in the shape of the pulse height distribution curves were noted. These distinct variations in Barkhausen noise signal observed prior to macroscopic yielding indicate the presence of microyielding.

References

1. D. L. ATHERTON and D. C. JILES, *NDT & E Int.* **18**(1) (1986) 15.
2. R. BECKER, *Physik. Z.* **33** (1932) 905.
3. R. M. BOZORTH, "Ferromagnetism" (IEEE Press, NY, 1951).
4. B. D. CULLITY, "Introduction to Magnetic Materials" (Addison-Wesley Publishing Co., Inc., NY, 1972).
5. W. L. DONALDSON and R. L. PASLEY, in Proceedings of the 6th Symposium on Nondestructive Evaluation of Aerospace and Weapons Components and Materials, Los Angeles (Western Periodicals Co., 1967) p. 563.
6. L. P. KARJALAINEN and M. MOILANEN, *IEEE Trans. Magn.* **MAG-16**(3) (1980) 514.
7. C. JAGADISH, L. CLAPHAM and D. L. ATHERTON, *ibid.* **25**(5) (1989) 3452.
8. *Idem., J. Phys. D: Appl. Phys.* **23** (1990) 443.
9. D. G. HWANG and H. C. KIM, *ibid.* **21** (1988) 1807.
10. R. BECKER and W. DÖRING, "Ferromagnetism" (Springer Verlag, Berlin, 1939).
11. T. W. KRAUSE, L. CLAPHAM, A. PATTANTYUS and D. L. ATHERTON, *J. Appl. Phys.* **79**(8) (1996) 4242.
12. G. BERTOTTI, *IEEE Trans. Magn.* **24** (1988) 621.
13. P. MAZZETTI and G. MONTALENTI, in Proceedings of the International Conference on Magnetism, Nottingham, 1964, p. 701.

14. M. CELASCO, F. FIORILLO and P. MAZZETTI, *Nuovo Cimento* B **23**(N2) (1974) 349.
15. H. BITTEL, *IEEE Trans. Magn.* **MAG-5** (1969) 359.
16. C. KITTEL and J. K. GALT, *Solid State Phys.* **3** (1956) 437.
17. E. W. LEE, *Rep. Prog. Phys.* **18** (1955) 184.
18. J. P. HIRTH, *Met. Trans.* **3** (1972) 3047.
19. M. A. MEYERS and K. K. CHAWLA, "Mechanical Metallurgy: Principles and Applications" (Prentice-Hall Inc., New Jersey, 1984).
20. L. E. MURR, *Met. Trans.* **6A** (1975) 427.
21. K. TANGRI and T. MALIS, *Surface Sci.* **31** (1972) 101.
22. W. D. BRENTNALL and W. ROSTOKER, *Acta Met.* **13** (1965) 187.
23. R. M. DOUTHWAITE and J. T. EVANS, *ibid.* **21** (1973) 525.
24. J. C. SUITS and B. CHALMERS, *ibid.* **9** (1961) 854.
25. P. J. WORTHINGTON and E. SMITH, *ibid.* **12** (1964) 1277.
26. M. A. MEYERS and E. ASHWORTH, *Phil. Mag. A* **46**(5) (1982) 737.
27. G. E. DIETER, JR., *Mechanical Metallurgy* (McGraw-Hill, Inc., NY, 1961).

Received 5 August
and accepted 11 November 1999